

Halogen-Free Flame-Retardant Waterborne Polyurethane with a Novel Cyclic Structure of Phosphorus–Nitrogen Synergistic Flame Retardant

Limin Gu,^{1,2} Zhen Ge,¹ Muhua Huang,¹ Yunjun Luo¹

¹School of Materials Science and Engineering, Beijing Institute of Technology, Haidian District, Beijing 100081, China

²School of Chemical and Pharmaceutical Engineering, Hebei University of Science and Technology, Shi Jiazhuang, Hebei Province 050018, China

Correspondence to: Y. Luo (E-mail: yjluo@bit.edu.cn)

ABSTRACT: A novel phosphorus–nitrogen flame retardant, octahydro-2,7-di(N,N-dimethylamino)-1,6,3,8,2,7-dioxadiazadiphosphocine (ODDP), with bi-phosphonyl in a cyclic compound, was synthesized by the reaction of POCl₃, NH(CH₃)₂·HCl with OHCH₂CH₂NH₂ in CH₂Cl₂ solution, and characterized by Fourier transform infrared spectrometer, nuclear magnetic resonance, and mass spectrum. ODDP has been successfully reacted with polyurethane (PU) as a chain extender to prepare phosphorus–nitrogen synergistic halogen-free flame-retardant waterborne PU (DPWPU). Limiting oxygen index (LOI), UL-94, thermogravimetric analysis and scanning electron microscopy suggest the excellent flame retardancy of the DPWPU polymer. When the content of ODDP was 15 wt %, the LOI of DPWPU was 30.6% and UL-94 achieved a V-0 classification. Compared with the unmodified WPU, the thermodecomposition temperature of the DPWPU was reduced and the amount of carbon residue was increased to 18.18%. The surface of carbon residue was shown to be compact and smooth without holes, which would be favorable for resisting oxygen and heat. © 2014 Wiley Periodicals, Inc. *J. Appl. Polym. Sci.* **2015**, *132*, 41288.

KEYWORDS: flame retardance; functionalization of polymers; polyurethanes; thermogravimetric analysis

Received 2 April 2014; accepted 10 July 2014

DOI: 10.1002/app.41288

INTRODUCTION

Cotton fabrics flame retardants are mostly halogen-containing compounds.¹ The widely used halogen-based retardants are not ecofriendly because the generated highly toxic gases can be harmful to human health.² The production of two major class bromine-based retardants, polybrominated diphenyl ethers (PBDEs) and polybrominated biphenyl (PBB), has been banned in Europe and the US.³ Evidence showed that PBDEs would persist in the environment and accumulate in the living organisms. Toxicological testing results indicated that these chemicals could cause liver, thyroid, and neurodevelopmental toxicity. Moreover, the Department of Health and Human Services and the International Agency for Research on Cancer suggested that PBBs could be carcinogenic to human health. During the past three decades, phosphorus–nitrogen (P–N) containing flame retardant systems have attracted much attention and have been widely investigated, primarily due to their good thermal stability and superior performance, resulting from the synergistic effect of P–N.^{4,5} P–N synergism is not a general phenomenon in any P–N containing compounds, and it depends on the polymer

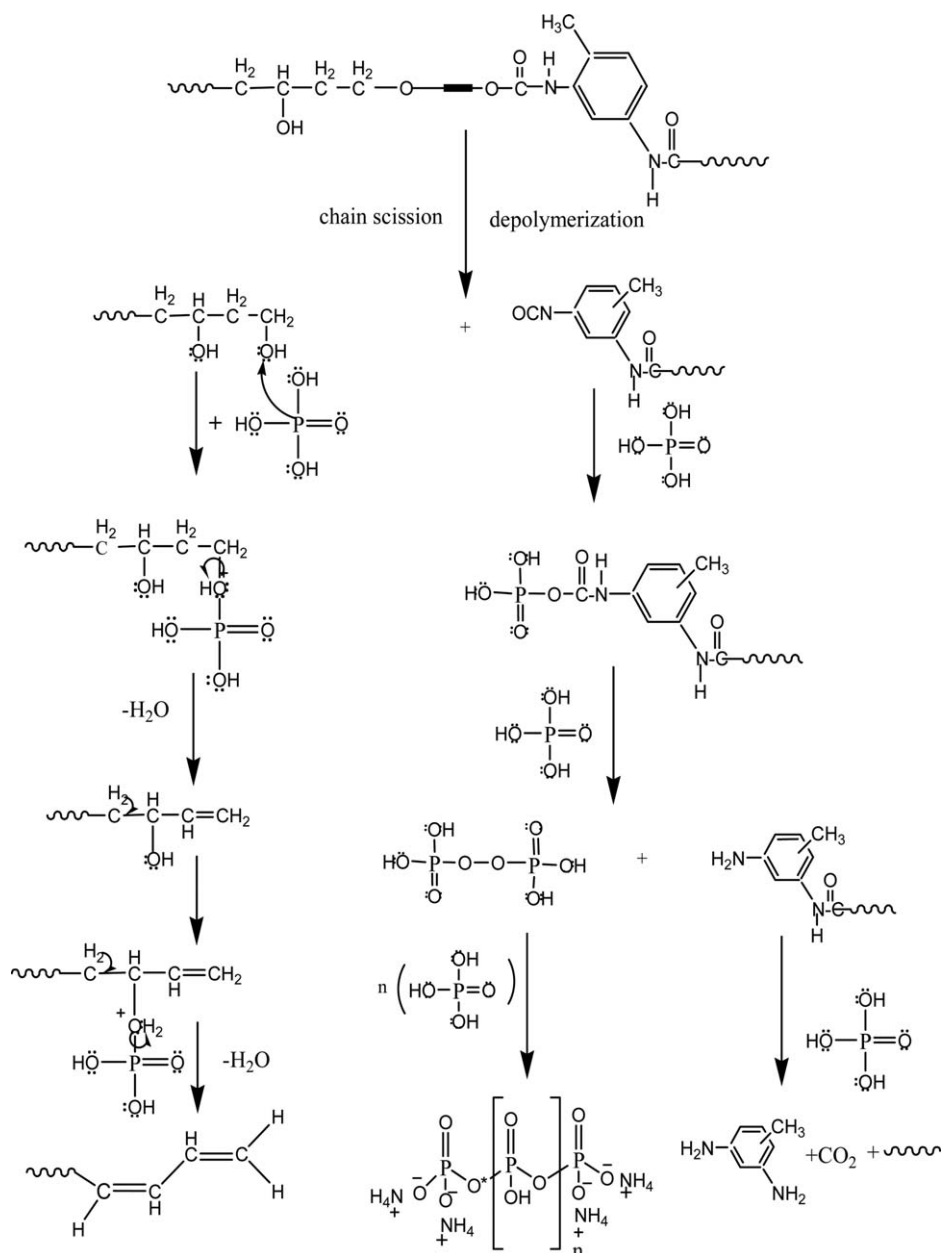
nature of the particular nitrogen containing compound. Several theories⁶ have been proposed to explain the synergistic effect of P–N systems resulted from reducing the formation of flammable volatiles as well as catalyzing char formation.

Waterborne polyurethane (WPU) presents many advantages compared to the conventional solvent borne polyurethanes, including its low viscosity at high molecular weight and good applicability, as well as its wide application to fabric coating. Recently, more and more studies have been carried out on flame retardant WPU.⁷ At present, most of the P–N synergistic flame retardants are alcohol compounds, and the products they reacting with isocyanate have bad influences on the mechanical properties of WPU. By contrast, the polyurea, which is the product of diamine reacting with isocyanate, shows better mechanical properties. Sheth et al.⁸ found that the degree of microphase separation was greater in the polyurea samples due to their more cohesive bidentate hydrogen bonding.

In this study, we first designed and developed a novel diamine with cyclic structure, which was a halogen-free P–N synergistic flame retardant: octahydro-2,7-di(N,N-dimethylamino)-1,6,3,8,2,7-dioxadiazadiphosphocine (ODDP), which possesses bi-phosphonyl

Additional Supporting Information may be found in the online version of this article.

© 2014 Wiley Periodicals, Inc.



Scheme 1. A simplified diagram of phosphoric acid dehydration and char formation mechanism of the PU.

in ringed formula structure. Bifunctionality was introduced to increase the number of reactive sites on the monomer to furnish better durability coupled with good flame retardancy due to P–N synergism. Second, a P–N synergistic halogen-free flame-retardant WPU (DPWPU) was prepared by reacting the ODDP with the prepolymer of PU molecular chains as hard segments. Characterization techniques such as limiting oxygen index (LOI), scanning electron microscopy (SEM), thermal gravimetric analysis (TGA), and differential scanning calorimetry (DSC) were used to investigate the thermal stability and fire retardancy.

EXPERIMENTAL

Materials and Reagents

The following chemicals were used as obtained from Beijing Yili fine chemicals (China) without further treatment: dichlorome-

thane (CH_2Cl_2), dimethylamine hydrochloride ($\text{NH}(\text{CH}_3)_2\text{HCl}$), ethanolamine (MEA), triethylamine (TEA), and butanone (MEK). Phosphorus oxychloride (POCl_3), polyether polyols (PPG1000, OH content 99.1 mg KOH/g, molecular weight: 1000), toluene diisocyanate (TDI 80/20) and 2,2-Bis(hydroxymethyl)propionic acid (DMPA) were purchased from Kelun chemicals (China), Third Oil Refinery of Tianjin Petrochemical (China), Shanghai Polyurethane Products Factory (China), and Beijing Linshi Chemical Industrial (China), respectively.

Synthesis of ODDP (Flame Retardant Monomer)

CH_2Cl_2 (50 mL) was added into a 250-mL three-neck round bottom flask containing a magnetic stir bar. Then, POCl_3 (0.15 mol) and $\text{NH}(\text{CH}_3)_2\text{HCl}$ (0.1 mol) were added into the flask, and triethylamine (0.15 mol), diluted in CH_2Cl_2 (50 mL),

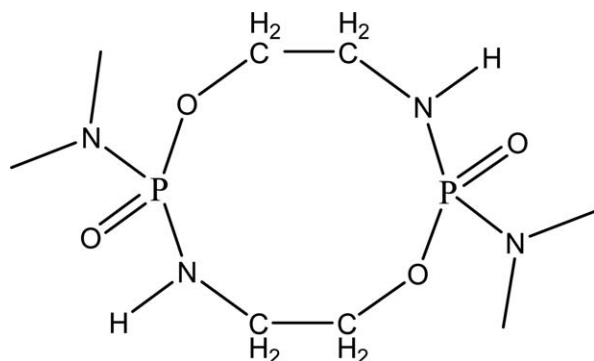


Figure 1. Phosphoramidate monomer with ringed structure synthesized in the study.

was dropped into the system within 1 h as acid binding agent. This reaction mixture was allowed to run at -5°C for 1 h, then at room temperature for 4 h to give triethylamine hydrochloride as a precipitate.

The precipitated triethylamine hydrochloride salt was removed by vacuum filtration, and the filtrate was then used for the next step. The filtrate from Step 1 was transferred into a clean three-neck round bottom flask. To the filtrate, triethylamine (0.15 mol) was added, and the three-neck flask was then connected to an inlet for N_2 , and an addition funnel, and the reaction mixture was cooled to 0°C . To the reaction mixture, ethanolamine (0.075 mol) dissolved in CH_2Cl_2 (50 mL) was added dropwise, and the reaction mixture was allowed to stay at 0°C for 2 h, then 40°C for 2 h. After, the reaction mixture was filtered by vacuum filtration to remove triethylamine hydrochloride precipitate, and the filtrate was washed with petroleum several times. Then, the filtrate was dried over MgSO_4 . At last, decompressing and distilling the filtrate to get the final product of ODDP ($\text{C}_8\text{H}_{22}\text{P}_2\text{N}_4\text{O}_4$, $M = 300$, white or pale yellow solid), with a yield of 46%. The reaction showing the synthesis of ODDP is shown in Supporting Information Scheme S1. The structural formula of the compound is shown in Figure 1.

Preparation of PU (Prepolymer)

The prepolymer of PU was prepared by using 18 g of TDI, 21 g of PPG1000, and 3 g of DMPA with 3 h mechanical stirring at 85°C .

Preparation of DPWPU (Flame-Retardant Polymer)

The P–N synergistic halogen-free flame-retardant WPU flame-retardant (DPWPU) was prepared in three steps based on the prepared prepolymer of PU. Take DPWPU15 (ODDP content is 15 wt %), for example: first, following the reaction of preparing the prepolymer of PU, the reaction temperature was increased to 90°C , and the chain-extender ODDP (7.5 g) was added. Second, after 4 h, the reaction temperature was decreased to 40°C , and the TEA (2.0 g) was added in the reaction system; finally, after 10 min, the reaction mixture reacted with water (150 g) under high-speed shearing for 3–5 min, and the DPWPU was obtained. This reaction conditions are as follows: $\text{NCO} : \text{OH}$ (mol : mol) = 1.4 : 1, neutralization = 90%, solid content = 25 wt %, ODDP content = wt 15%. Supporting Information

Scheme S2 depicts the whole preparation process of DPWPU15 synthesis (Supporting Information).

Characterization

FTIR. Fourier transform infrared spectrometer (FTIR) spectra of the ODDP, prepolymer of PU and DPWPU samples embedded in KBr pellets were recorded on a Nicolet FTIR 170SX spectrometer over the wavenumber range from 500 to 4000 cm^{-1} at room temperature. (The latex film needed to be swelling in acetone for 48 h before testing.)

$^1\text{H NMR}$. $^1\text{H NMR}$ was obtained on a Jeol nuclear magnetic resonance (NMR) EX-270.

$^{13}\text{C NMR}$. $^{13}\text{C NMR}$ was obtained on a Jeol NMR EX-270.

Elementary Analysis. ICP-AES was used to measure the actual phosphorus content, and the contents of nitrogen, carbon, and hydrogen were measured by VarioELcube.

Mass Spectrum. Mass spectrum was measured using Finnegan Mat SSQ 700 (England).

Morphologies of Char. The morphology of various char samples after DPWPU combustion was captured by an INSPECTF SEM at the accelerating voltage of 15 kV. The surfaces of char samples were coated with a thin gold layer before observation.

LOI. LOI tests were performed at room temperature using a HC-2C oxygen index instrument based on ISO 4589-1984. The size of the specimen was $150 \times 50 \times 3\text{ mm}^3$ (length \times width \times thickness).

UL-94 Vertical Burning Test. The vertical burning test was conducted by a CZF-II horizontal and vertical burning tester (Jiang Ning Analysis Instrument). The specimens used were $127 \times 12.7 \times 3\text{ mm}^3$ according to the UL-94 test (ASTM D3801-1996 standard).

TGA. TGA was performed using METTLER TGA/DSC1, with a heating rate of $10^{\circ}\text{C}/\text{min}$ and N_2 as the shielding gas. The temperature range was $30\text{--}600^{\circ}\text{C}$.

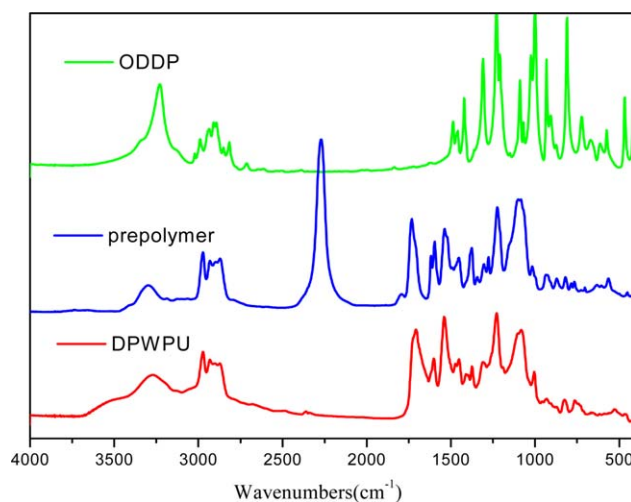


Figure 2. The FTIR spectra for ODDP, prepolymer of PU and DPWPU. [Color figure can be viewed in the online issue, which is available at wileyonlinelibrary.com.]

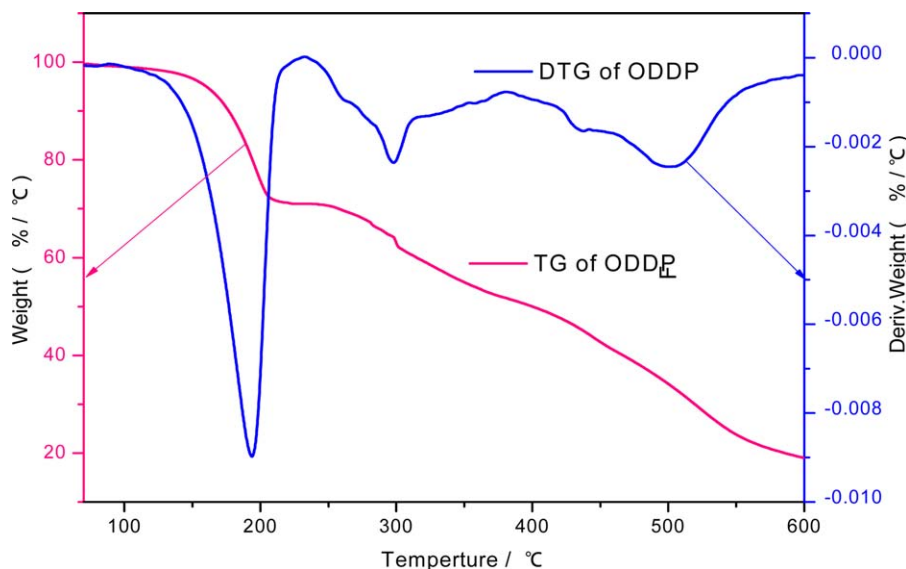


Figure 3. TG/DTG thermogram of ODDP under a N_2 atmosphere. [Color figure can be viewed in the online issue, which is available at wileyonlinelibrary.com.]

TG/FTIR. The TGA/FTIR experiments were performed using a thermal analyzer system coupled with a FTIR. TGA (TGA/DSC1SF/ 417-2, Mettler Toledo) used a heat rate of $10^\circ\text{C}/\text{min}$ from 30 to 600°C and N_2 as the shielding gas. FTIR (Nicolet IS10, Thermo) was linked to the TGA to measure the gas products. The gas lines between the TGA and the FTIR were heated to 220°C . The spectra were collected at a resolution of 4 cm^{-1} .

DSC. The glass transient temperature was determined by METTLER TOLEDO DSC1, and the heating rate was $10^\circ\text{C}/\text{min}$. N_2 was used as the shielding gas and the temperature range was -100 – $120^\circ\text{C}/\text{min}$.

RESULTS AND DISCUSSION

Characterization

Characterization of ODDP. The structure of ODDP was characterized by FTIR, $^1\text{H-NMR}$, $^{13}\text{C-NMR}$, elemental analysis and mass spectrometry. The FTIR spectrum (Figure 2: line 1) presents the absorption peaks at 3264 cm^{-1} , 2930 – 2894 cm^{-1} , and 1394 cm^{-1} , which should correspond to $-\text{NH}$, $-\text{CH}_2-\text{CH}_2$, and $-\text{P}-\text{NH}$, respectively. In addition, the peaks at 1213.99 cm^{-1} , 1310.41 cm^{-1} , and 1004 cm^{-1} should be attributed to $\text{P}=\text{O}$, $-\text{N}-\text{C}$, and $-\text{P}-\text{N}$, respectively. The $^1\text{H-NMR}$ (Supporting Information Figure S1) shows that the product has a $-\text{NH}-$ proton which appeared as a shoulder

peak at 2.55 ppm along with four sets of multiplets at 3.3 and 3.5 ppm as well as 4.1 and 4.3 ppm assignable to $-\text{N}-\text{CH}_2$ and $-\text{O}-\text{CH}_2$, respectively. Due to the carbon atoms embedded in molecular ring structure, the hydrogen which is attached to carbon shows multiple splitting. Further, the peak at 2.65 ppm splits into two main peaks, which are assignable to $\text{N}-\text{(CH}_3)_2$. According to the special symmetrical structure, the relative peak ratio of every characteristic peak is 1 : 1 : 1 : 1 : 6 : 1, which is identical to the target molecule. The $^{13}\text{C-NMR}$ (100 MHz, CDCl_3 , Supporting Information Figure S2) shows that the product (ODDP) has three kind of carbon, δ (ppm): 66.26, 42.34, 36.65 (77.11 ppm belongs to CDCl_3). The positive FAB-MS exhibits one pseudo molecular ion peak at m/z 323.1 of $[\text{M} + \text{Na}]^+$ (Supporting Information Figure S3). The results of elemental analysis are shown in Supporting Information Table S1. The actual contents of phosphorus, nitrogen, carbon, and hydrogen were almost coincident with their theoretical contents (The error between actual contents and theoretical contents less than 0.3%). Combined with the $^1\text{H-NMR}$ data, $^{13}\text{C-NMR}$, elemental analysis and mass spectrometry, it is concluded that the molecular formula of ODDP is $\text{C}_8\text{H}_{22}\text{P}_2\text{N}_4\text{O}_4$.

Characterization of DPWPU. The structures of prepolymer of PU and DPWPU were characterized by FTIR (Figure 2: lines 2

Table I. Flammability of DPWPU Containing Different Content of ODDP Compounds

Samples	ODDP (wt %)	P (wt %)	N (wt %)	LOI (%)	UL-94 classification
DPWPU0	0	0	0	25.4	V-2
DPWPU5	5	1.03	0.93	29.6	V-1
DPWPU10	10	2.07	1.87	30.2	V-0
DPWPU15	15	3.10	2.80	30.6	V-0
DPWPU20	20	4.13	3.73	29.8	V-0

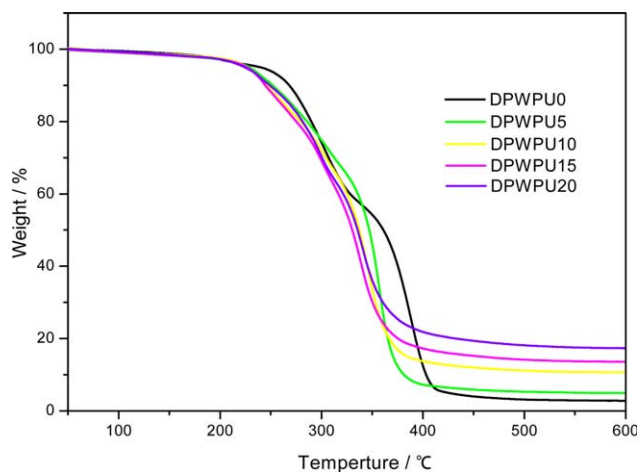


Figure 4. TG curves for DPWPU0, DPWPU5, DPWPU10, DPWPU15, DPWPU20 under N_2 atmosphere. [Color figure can be viewed in the online issue, which is available at wileyonlinelibrary.com.]

and 3). One can see from the FTIR spectra that the NCO-group remained at first, which shows on the spectrogram for prepolymer of PU (Figure 2: line 2), and they appeared at 2272 cm^{-1} . When ODDP effectively copolymerized with prepolymer of PU, the NCO-group peak disappeared (Figure 2: line 3). The FTIR absorption peaks for DPWPU appeared at 3264.5 cm^{-1} (N—H), 1721.1 cm^{-1} (C=O), 1674.9 cm^{-1} (C=O in secondary or tertiary amides), 1213.99 cm^{-1} (P=O), 1310.41 cm^{-1} , 1004.6 cm^{-1} , 742.1 cm^{-1} (P—N— $(\text{CH}_3)_2$), and 1103 cm^{-1} (C—O—C).^{9–11}

Thermal Degradation Behavior of ODDP. The TG/DTG thermogram of ODDP under nitrogen atmosphere is shown in Figure 3. It can be seen that the decomposition of ODDP owned four main stages, in which the temperatures of maximum weight loss were found at 198.7, 300.1, 415.6, and 497.8°C, respectively. The 5% weight loss temperature ($T_{5\%}$) of ODDP was 160.8°C, and the amount of residue (char yield) at 600°C was 19.8%.

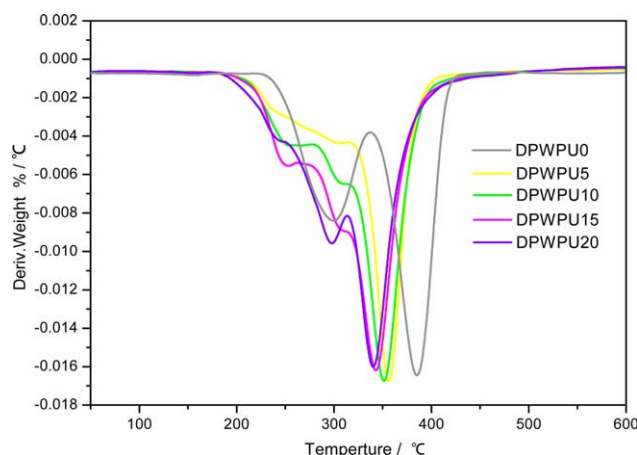


Figure 5. DTG curves for DPWPU0, DPWPU5, DPWPU10, DPWPU15, DPWPU20 under N_2 atmosphere. [Color figure can be viewed in the online issue, which is available at wileyonlinelibrary.com.]

Flammability Test

The major task for a flame retardant is preventing or delaying flashover from the surface of combustibles; therefore, a flame retardant is not designed to prevent the polymer from ignition but to minimize the flame spread rate and prevent sustained burning.^{12,13} The flame-retardant properties of DPWPU modified with ODDP are characterized by LOI and UL-94 as shown in Table I.

It was observed that the LOI values of DPWPU increased with the increase of ODDP contents when the content of ODDP is less than or equal to 15 wt %. The LOI value of DPWPU is 30.6% when the ODDP content increased to 15 wt %, implying flame retardant materials according to Fire Resistance Class Rating. There are two key reasons for the high LOI value of DPWPU. On the one hand, the flame retardant ODDP starts breaking down at low temperatures, and one of the thermodecomposition residues of ODDP is phosphoric acid. The presence of phosphorus-based flame retardant alters the pyrolysis path of the substrate by lowering the decomposition temperature, eventually reducing the formation of gaseous combustibles and favors the formation of char. On the other hand, ODDP has a high content of nitrogen, resulting in the enhancement of P—N synergistic effect.¹⁴ In this case, more noncombustible gases are produced, which is due to the dilution effect of ammonia. More noncombustible gases decomposed from ODDP on the oxygen concentration surrounding DPWPU, and they can act as gas phase flame retardant. But, when the ODDP content increased to 20 wt %, the LOI value of DPWPU is decreased. This is maybe because the flame retardant ODDP starts breaking down at low temperatures, and the degradation of flame-retardant DPWPU at 189–260°C is attributed to the initial weight loss of ODDP. With the increase of ODDP contents in DPWPU, the initial degradation part of DPWPU became more and more (Figure 5). On the other hand, a part of ODDP have completely decomposed and disappeared before depolymerization of PU to form isocyanate and polyol when the content of ODDP is 20 wt %, and this part of ODDP plays no role in inflaming retarding.

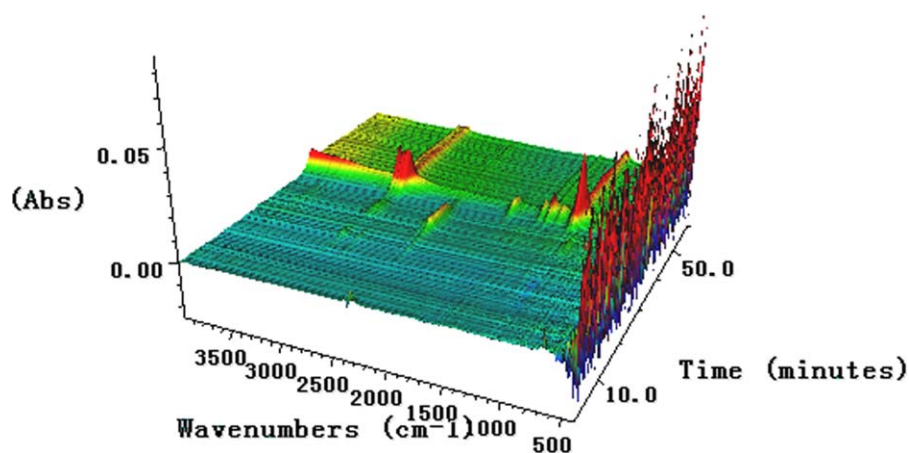
Furthermore, the testing results of UL-94 show that DPWPU10, DPWPU15, and DPWPU20 achieve a V-0 classification, which is due to the increase of the phosphorus content in polymer.¹⁵ In all, LOI and UL-94 testing results show a significant improvement in fire resistance in the presence of ODDP in DPWPU polymer.

Thermal Gravimetric Analysis

Figures 4 and 5 show the TG and DTG curves of DPWPU. It is reported that the thermal degradation of PUs occurs in a two- to three-step process.^{16,17} Figures 4 and 5 show that the DPWPU0 has a two-step degradation process at 231–342°C (hard segments) and 342–448°C (soft segments), respectively. However, the decomposition of flame-retardant DPWPU take place at three stages, 160–260°C (flame retardant), 260–330°C (hard segments), and 309–405°C (soft segments), respectively. The second and the third degradation processes of flame-retardant DPWPU are in accordance with the degradation processes of the DPWPU0. The degradation of flame-retardant

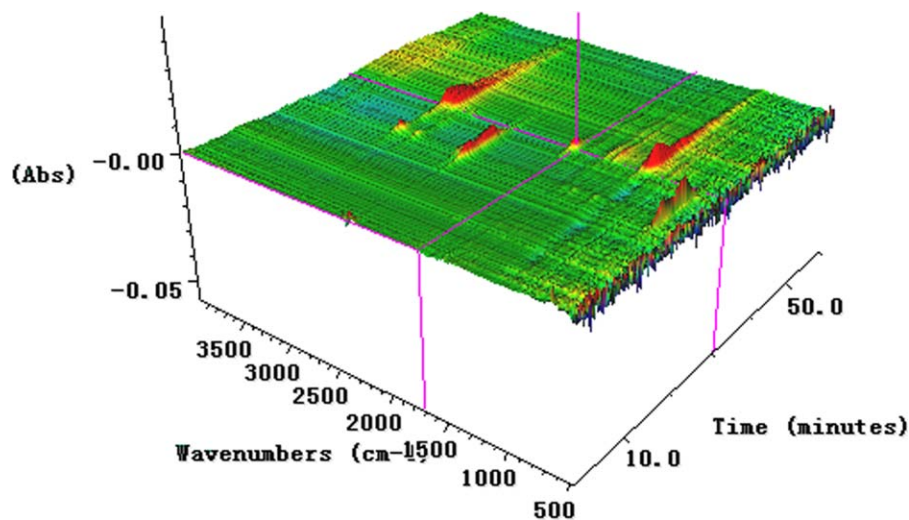
Table II. Data of TGA

Samples	DPWPU0	DPWPU5	DPWPU10	DPWPU15	DPWPU20
$T_{5\%}/^{\circ}\text{C}$	245.6	218.3	214.3	213.1	208.2
$T_{\text{max}1}/^{\circ}\text{C}$	-	237.8	230.1	227.3	225.9
$T_{\text{max}2}/^{\circ}\text{C}$	301.7	305.7	302.8	301.2	298.1
$T_{\text{max}3}/^{\circ}\text{C}$	387.4	356.3	351.2	344.8	343.6
Char yield(480 $^{\circ}\text{C}$)%	3.06	5.48	10.86	14.45	18.18

**Figure 6.** 3D TGA-FTIR spectra of decomposition products of DPWPU0 during the thermal degradation under N_2 atmosphere. [Color figure can be viewed in the online issue, which is available at wileyonlinelibrary.com.]

DPWPU at 189–260 $^{\circ}\text{C}$ was attributed to the initial weight loss of ODDP. With the increase of ODDP contents in DPWPU, the initial degradation peak of DPWPU5–DPWPU20 became wider and wider (Figure 5). The second degradation step is mainly due to the depolymerization of PU (hard segments) to form isocyanate, polyol, primary or secondary amine, olefin, and carbon dioxide.¹⁸ The third degradation step at 309–405 $^{\circ}\text{C}$ is

caused by the decomposition of the DPWPU without ODDP (soft segments) and ODDP. Table II shows the detailed thermal decomposition temperatures of samples determined from Figures 3 and 4. We can see clearly that with the increase of ODDP wt %, there is a decrease of the onset decomposition temperature ($T_{5\%}$), the first maximum weight loss temperature ($T_{\text{max}1}$), the second and third maximum weight loss

**Figure 7.** 3D TGA-FTIR spectra of decomposition products of DPWPU15 during the thermal degradation under N_2 atmosphere. [Color figure can be viewed in the online issue, which is available at wileyonlinelibrary.com.]

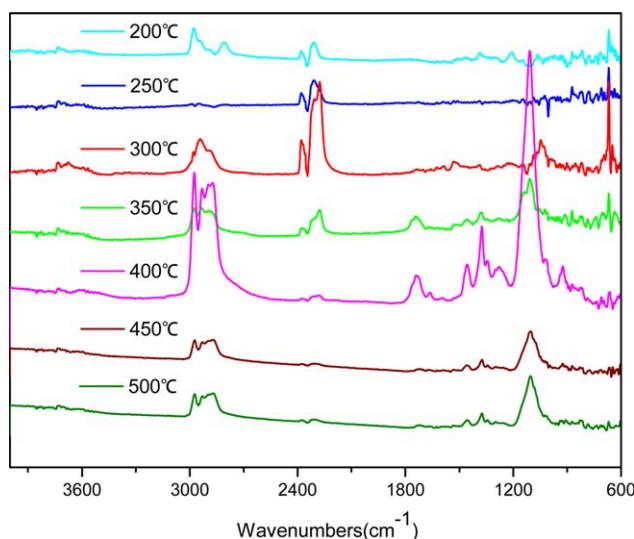


Figure 8. FTIR spectra of volatile products at representative temperature during thermal degradation of DPWPU0. [Color figure can be viewed in the online issue, which is available at wileyonlinelibrary.com.]

temperature ($T_{\max 2}$ and $T_{\max 3}$). The variation of $T_{\max 1}$ is related to the thermal stability of ODDP in this temperature range. The decrease of $T_{5\%}$, $T_{\max 2}$, and $T_{\max 3}$ is attributed to the breakage of the ODDP and formation of polyphosphoric acid, which will accelerate the decomposition of flame-retardant ODDP as a strong catalyst.

As far as the residue is concerned, it is found that the char residue at 480°C is increased with the increase of ODDP contents (Table II). This proved that the phosphorus and nitrogen in ODDP may have a synergistic effect on char formation, which can help to improve the flame retardancy of DPWPU. Besides this, ODDP can form phosphoric anhydrides or the related acids at higher decomposition temperature, and these resultants also promote the char formation. Researchers report that, phosphoric acid and polyphosphoric acids are produced by decomposition of P–N flame retardant, and they are catalyst for the char formation and dehydration of polyhydric alcohol^{19,20} as shown in Scheme 1.

TGA/FTIR Analysis

TGA analysis has proven to be a very useful technique for studying the thermal behavior of a wide variety of solid samples. However, TGA analysis by itself does not identify the decomposition products. When TGA analysis is coupled with evolved gas analysis, a great deal of additional information can be obtained. The TGA-FTIR spectra of decomposition products of DPWPU0 and DPWPU15 during the thermal degradation are shown in Figures 6 and 7. It should be noted that the peaks are shifted to a higher temperature than the corresponding DTG curve due to the delay time between the gas generation and its detection by the FTIR equipment. The FTIR spectra of gas products during decomposition at respective peaks are presented in Figure 8 and 9. As shown in Figure 7, CO_2 (2250–2400 cm^{-1}) release during 250–350°C, and CO (1726 cm^{-1}) is emitted at 350°C. Besides, the gas products of DPWPU0 at 400°C are identified as CH_2O ,

or $\text{C}_2\text{H}_4\text{O}$, or their mixture (1000–1202 cm^{-1} , 1718–1773 cm^{-1} , 2750–3010 cm^{-1}). As shown in Figure 9, the evolved gases for DPWPU15 contain, in addition to the decomposition products of DPWPU0, other new nonflammable gas products such as NH_3 (960, 929 cm^{-1}) and CO_2 (2250–2400 cm^{-1}). In contrast, CO (1726 cm^{-1}) disappeared at 400°C. The release of new compounds from decomposition DPWPU15 and vanish of characteristic absorption peaks of CO at 400°C may suggest that the flame retardant can influence the thermal decomposition of DPWPU. Furthermore, the peak intensity of the pyrolysis products from DPWPU15 is much lower than that from DPWPU0, especially for hydrocarbons and aromatic compounds. Consequently, the addition of intumescent flame retardant obviously reduces the release of combustible gases and the loss of weight. From the TG and TG-FTIR studies, it could be concluded that the ODDP can catalyze the formation of a protective char layer and the release of nonflammable gas leading to expansion of the layer. This expanded char layer could inhibit heat transmission and heat diffusion effectively.

Morphologies of Char

The morphologies of various char samples are shown in Figure 10. The morphology of DPWPU0 char is puffed and poriferous (Figure 10: A and A₁). By contrast, the morphology of DPWPU15 char is smooth and very dense as shown in Figure 10: B and B₁. The char with a smooth and very dense surface can act as a barrier to heat, air/ O_2 , and pyrolysis products.²¹ This is another evidence showing that DPWPU has good flame retardancy. The morphology of char samples consolidated the study of char yield (480°C) of DPWPU.

Analysis of DSC

The DSC thermograms of the DPWPU films are shown in Figure 11. All DPWPU samples show two glass transition temperatures: The glass transition temperature of soft segments (T_{gs}) and the glass transition temperature of hard segments (T_{gh}).

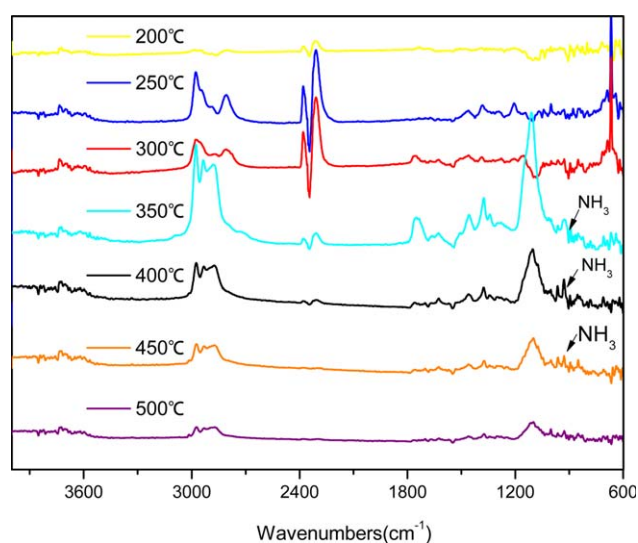


Figure 9. FTIR spectra of volatile products at representative temperature during thermal degradation of DPWPU15. [Color figure can be viewed in the online issue, which is available at wileyonlinelibrary.com.]

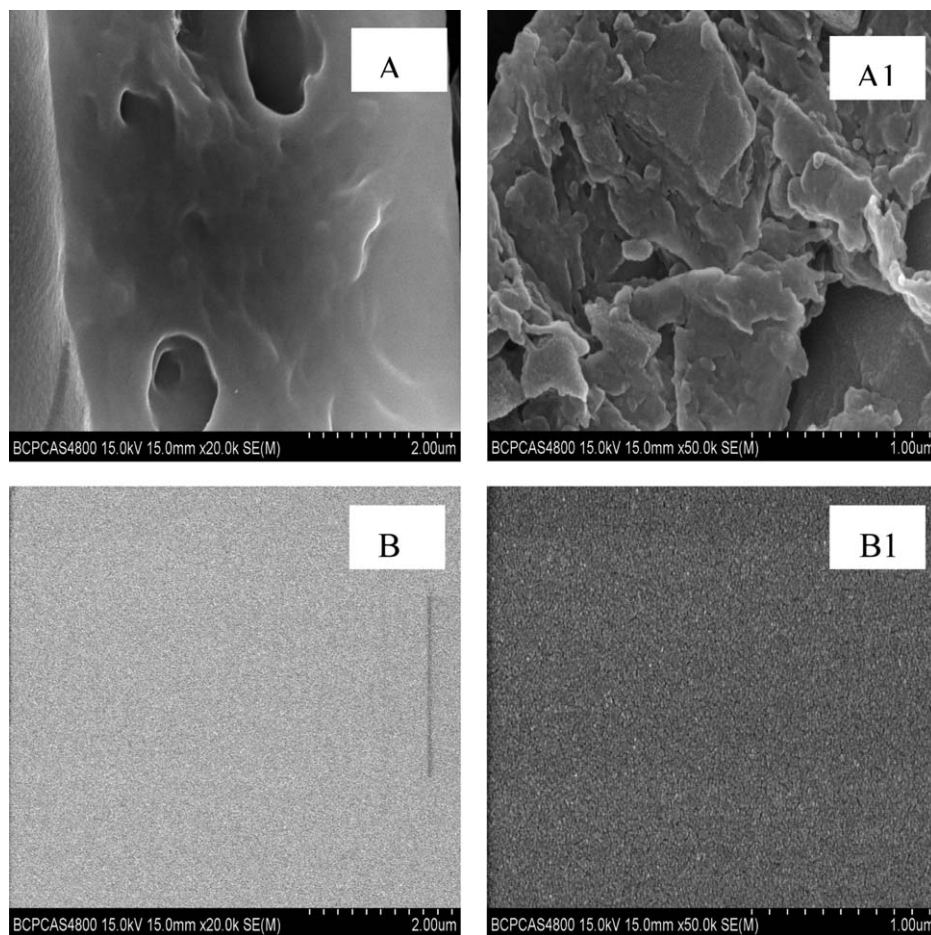


Figure 10. SEM monographs [A: DPWPU0(20K) and A1: DPWPU0(50K), B: DPWPU15(20K) and B1: DPWPU15(50K), respectively].

The data of DSC are shown in Table III, and we can see from Table III that the T_{gh} value decreases with the increase of ODDP contents. The decrease of T_{gh} value is mainly due to the

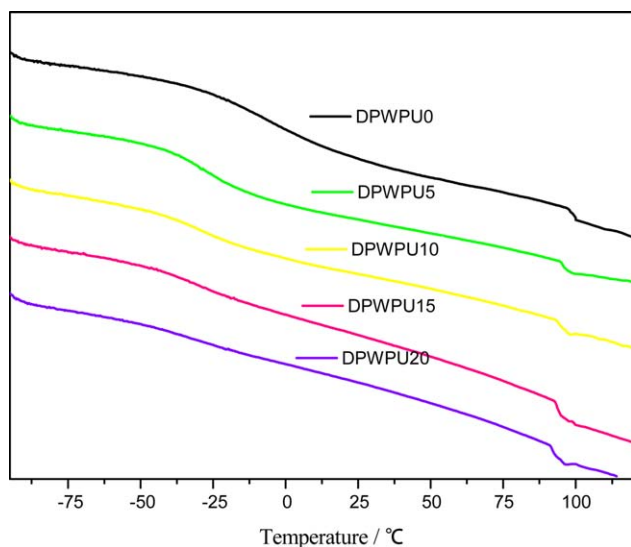


Figure 11. DSC curves of DPWPU. [Color figure can be viewed in the online issue, which is available at wileyonlinelibrary.com.]

ten-membered ring structure of ODDP, which increases the space between the molecular chains and reduces the intermolecular forces.²² Further, when the ODDP content from 5% up to 10%, the T_{gs} increased and T_{gh} decreased. In this stage, the hard segment will provide more physical crosslinking through hydrogen bonding. This increase can be attributed to the restricted mobility of the polymer chains as a result of the ten-membered ring structure of ODDP, leading to a better microphase separation degree of the system.²³ However, when the ODDP content is greater than 10%, the hard segment content of DPWPU is greater than 50%, and the hard segment is a continuous phase, so the ΔT_g increased, and microphase separation degree increases.

Table III. Data of DSC

Samples	T_{gs} (°C)	T_{gh} (°C)	ΔT_g (°C)
DPWPU0	-33.66	96.85	130.51
DPWPU5	-45.46	95.44	140.90
DPWPU10	-32.27	94.08	126.35
DPWPU15	-37.44	93.78	131.22
DPWPU20	-42.76	93.07	135.83

CONCLUSIONS

ODDP has been synthesized via the reaction of POCl_3 , $\text{NH}(\text{CH}_3)_2 \cdot \text{HCl}$ with MEA. The molecular structure of ODDP has been confirmed by FTIR, ^1H NMR, ^{13}C NMR, elemental analysis and Mass spectrum. FTIR, TGA, LOI, UL-94, SEM, and DSC results suggest that DPWPU was first successfully prepared from the reaction of ODDP with the WPU molecular chains as a chain extender. DPWPU has excellent flame retardancy, which is attributed to the presence of ODDP. The nitrogen atoms of ODDP increase the P–N synergistic effect, resulting in more thermally stable and highly cross linked matrix residue, which holds the material fragments in the condensed phase for longer time, thus furnishing more and integrated charring. In addition, due to the 10-membered ringed structure of ODDP, the micro-phase separation degree of DPWPU was increased, thus the high-temperature thermal endurance property of polymers was enhanced. The LOI value of DPWPU is 30.6% and UL-94 achieves a V-0 classification as the ODDP content increases to 15 wt %. According to Fire Resistance Class Rating, it reaches the grade level where it is difficult to burn.

REFERENCES

1. Hammad, A. C.; Ahmed E.-S.; Peter, J. H. *Carbohydr. Polym.* **2013**, *92*, 885.
2. Sabyasachi, G.; Gang, S. *Polym. Degrad. Stab.* **2007**, *92*, 968.
3. Gaan, S.; Sun, G.; Hutches, K.; Engelhard, M. H. *Polym. Degrad. Stab.* **2008**, *93*, 99.
4. Konig, A.; Kroke, E. *Polym. Adv. Technol.* **2011**, *22*, 5.
5. Jeng, R. J.; Shau, S. M.; Lin, J. J.; Su, W. C.; Chiu, Y. *Eur. Polym. J.* **2002**, *38*, 683.
6. Horacek, H.; Grabner, R. *Polym. Degrad. Stab.* **1996**, *54*, 205.
7. Lefebvre, J.; Bastin, B.; Bras, M. L.; Duquesne, S.; Ritter, C.; Paleja, R.; Poutch, F. *Polym. Test* **2004**, *23*, 281.
8. Sheth, J. P.; Aneja, A.; Wilkes, G. L.; Yilgor, E.; Atillab, G. E.; Yilgorb, I.; Beyer, F. L. *Polymer* **2004**, *45*, 6919.
9. Luo, Y.; Li, J.; Chen, H.; Ge, Z.; Li, X. China Pat. CN200810172238.7, October 31, 2008.
10. Luo, Y.; Li, J.; Chen, H.; Ge, Z.; Li, X. China Pat. ZL200810172239.1, October 31, 2008.
11. Luo, Y.; Li, X.; Li, F. China Pat. N201010516243.2, October 22, 2010.
12. Ming-Jun, C.; Zhu-Bao, S.; Xiu-Li, W.; Li, C.; Yu-Zhong, W. *Ind. Eng. Chem. Res.* **2012**, *51*, 9774.
13. Bian, X. C.; Tang, J. H.; Li, Z. M.; Lu, Z. Y.; Lu, A. *J. Appl. Polym. Sci.* **2007**, *104*, 3347.
14. Horacek, H.; Grabner, R. *Polym. Degrad. Stab.* **1996**, *54*, 205.
15. Matthias, N.; Shuyu, L.; Henri, M.; Sabyasachi, G. *Ind. Eng. Chem. Res.* **2013**, *52*, 9752.
16. Petrovic, Z. S.; Zavargo, Z.; Flynn, J. H.; Macknight, W. J. *J. Appl. Polym. Sci.* **1994**, *51*, 1087.
17. Zhang, L.; Jeon, H. K.; Malsam, J.; Herrington, R.; Macosko, C. W. *Polymer.* **2007**, *48*, 6656.
18. Ravey, M.; Pearce, E. M. *J. Appl. Polym. Sci.* **1997**, *63*, 47.
19. Price, D.; Liu, Y.; Milnes, G. J.; Hull, R.; Kandola, B. K.; Horrocks, A. R. *J. Fire Mater.* **2002**, *26*, 201.
20. Chattopadhyay, D. K.; Webster, D. C. *J. Prog. Polym. Sci.* **2009**, *34*, 1068.
21. Green, J. J. *Fire Sci.* **1996**, *14*, 426.
22. Chen, H.; Luo, Y.; Chai, C.; Li, J. *Polym. Mater. Sci. Eng.* **2008**, *24*, 90.
23. Lee, H. S.; Shaw, L. H. An analysis of phase separation kinetics of model polyurethanes. *Macromolecules* **1989**, *22*, 1100.